applied sciences

MDPI

Article

On the Determination of Acoustic Properties of Membrane Type Structural Skin Elements by Means of Surface Displacements

Daniel Urbán [1,2,*], N. B. Roozen [3], Vojtech Jandák [1], Marek Brothánek [1] and Ondřej Jiříček [1]

[1] Department of Physics, Faculty of Electrical Engineering, Czech Technical University in Prague, Technicka 2, 166 27 Prague, Czech Republic; jandav1@fel.cvut.cz (V.J.); brothan@fel.cvut.cz (M.B.); jiricek@fel.cvut.cz (O.J.)
[2] Department of Materials Engineering and Physics, Faculty of Civil Engineering, Slovak University of Technology in Bratislava, Radlinského 11, 810 05 Bratislava, Slovakia
[3] Department of Physics and Astronomy, Soft Matter and Biophysics, Laboratory of Acoustics, KU Leuven, Celestijnenlaan 200D, 3001 Leuven, Belgium; bert.roozen@kuleuven.be
* Correspondence: daniel.urban@stuba.sk

Abstract: The article focuses on the determination of the acoustic properties (sound transmission loss, sound absorption and transmission coefficient under acoustic plane wave excitation) of membrane-type of specimens by means of a combination of incident plane wave sound pressure and membrane surface displacement information, measuring the sound pressure with a microphone and the membrane displacement by means of a laser Doppler vibrometer. An overview of known measurement methods and the theoretical background of the proposed so-called mobility-based method (MM) is presented. The proposed method was compared with the conventional methods for sound transmission loss and absorption measurement in the impedance tube, both numerically and experimentally. Finite element model (FEM) simulation results of two single layer membrane samples of different shape configurations were compared, amongst which six different variations of the backing wall termination. Four different approaches to determine the sound transmission loss and two methods to determine sound absorption properties of the membranes were compared. Subsequently, the proposed method was tested in a laboratory environment. The proposed MM method can be possibly used to measure the vibro-acoustic properties of building parts in situ.

Keywords: membranes; acoustics; measurement method; transmission loss; simulations; experiment

Citation: Urbán, D.; Roozen, N.B.; Jandák, V.; Brothánek, M.; Jiříček, O. On the Determination of Acoustic Properties of Membrane Type Structural Skin Elements by Means of Surface Displacements. *Appl. Sci.* **2021**, *11*, 10357. https://doi.org/10.3390/app112110357

Academic Editor: Alessandro Ruggiero

Received: 29 September 2021
Accepted: 2 November 2021
Published: 4 November 2021

1. Introduction

The membranes of variable shape are used both indoors and outdoors where membranes have become part of roofing and shielding elements as well as of facades. A wide range of solutions for structural skins exists, whether for single, second skin or double skin facades, atria coating or exterior environment covering [1]. Moreover, lightweight solutions such as membrane-based constructions are considered as a sustainable solution in architecture [2]. From an acoustic point of view, every new construction solution brings specific pitfalls associated with it. For example, the impact of the frequently used double transparent facades (DTF) on administrative buildings for sound insulation improves the sound reduction index, but has possible negative effects in the low frequency range caused by standing wave resonances occurring in the air cavity inside the DTF. DTFs can also cause problems related to speech privacy in the interior caused by flanking transmission paths between attached offices, which can be problematic mainly in cases of low background noise level in the DTF cavity [3,4]. Nowadays, when the influence of facades on environmental noise is increasingly being discussed, adaptive facade (or smart façade-facades that adapt to the climate and environment through their skin) solutions with implemented membrane structures are a topic of growing interest. The properties of membrane structures are very dependent on their mass, dimensions and mechanical stresses. The present work was

motivated by the idea of Martens et al. [5], where authors investigated in the determination of the sound energy absorbed by the plant leaves based on the measured surface velocity and sound pressure. The goal was to verify it that would be possible to apply the proposed theory in an experimental way.

The theory of circular and annular membranes was described by Rayleigh [6]. For more complex shapes, several approximate methods have been proposed by Mazumdar [7]. Later, the impact of the circular core fixed to the membrane was investigated [8]. A number of previous works were published with a focus on the variations of the membrane boundary conditions. For example, Wang investigated the impact of a pinned large axisymmetric mass at the centre of the membrane on its natural frequency [9,10]. These kinds of membranes were also called membrane-type metamaterial (MAMs) with so-called negative dynamic mass [11–14].

By stacking together membrane panels with attached mass (circular shaped weights) in the centre of membrane surfaces, the sound transmission loss of the membrane composition can be increased in a broad band frequency range from 50 to 1000 [15]. The effect of the mass of the membrane and the membrane tension on the transmission loss was investigated by a number of researchers [15,16]. Normally, the bending stiffness of membranes can safely be ignored. The restoring force arises entirely from the applied tension, not from bending stiffness as is the case for plates.

Relatively popular MAMs or locally resonant sonic materials (LRSMs) contain arrays of elastic resonators composed of a heavy core surrounded by a soft coating layer. In principle, by loading the membrane by a relatively heavy object the so-called dipole resonance occurs. The dipole resonance enhances the acoustic performance [17,18]. These resonant materials are able to control low-frequency sound reflection and transmission very effectively. The negative dynamic mass causes the subwavelength attenuation of sound in the audible frequency band and breaks the mass density law. In the frequency range from 100 to 1000 Hz, a significant increase of the normal incidence sound transmission loss (*nTL*) can be achieved [19]. Spatially averaged force and acceleration are opposite in phase, which leads to near-total reflection (anti-resonance) at the frequency between two eigenmodes. In this region, the in-plane average of normal displacement is close to zero [19]. This finding is usually visible in the sound transmission loss *TL* (dB) spectra as a peak in the spectrum. Dips in *TL* and peaks in the sound absorption spectra are caused by symmetrical eigenmodes.

An analytical vibroacoustic membrane model as a tool for the design of MAMs was developed in [20]. Another analytical model was developed to compute the sound transmission loss of a mass loaded rectangular membrane in a fast manner. It was shown that the mass of the membrane is especially affecting the first normal incidence transmission loss (*nTL*) peak and the resonance frequency, while the second resonance frequency strongly depends on the membrane properties [21]. In the publication, the effects of the membrane tension and the membrane surface density on transmission and characteristic frequencies were investigated as well. Zhang later focused on the low-frequency sound attenuation by MAMs carrying different masses at adjacent cells [22]. However, the most universal tool to predict MAMs behaviour is still the Finite Element Analysis (FEA) approach (with a commonly accepted uncertainty of about 20 dB peaks and dips of transmission loss spectra. Additionally, the MAMs with coaxial ring masses were experimentally and numerically analysed. The multiple coaxial arranged rings resulted in multi-peak profile (uniform mass) or broadband *TL* peak (non-uniform mass) [19].

In later works, Naify investigated the scaling of LRSMs [23] by multi-celled structure analysis. The impact of two parallel cells with mass and air cavity was analysed. It appeared that the cavity thickness difference (from 2–4 mm) had a negligible effect on its normal incidence sound transmission loss (*nTL* (dB)) spectra in the frequency region below 1 kHz. It must be mentioned at this point, the applications based on MAMs principle can find the application not just in the membrane type constructions. By application the

dynamic vibration absorbers the significant local control of low-frequency noise can be achieved [24–27].

Overview of Measuring Methods

Most of the investigations were performed under the acoustic plane wave incidence conditions, by means of the Impedance Tube Method (ITM), also called the Standing Wave or Kundt's Tube Method. This measurement approach typically determines the *nTL* and sound absorption (α(-)) (or reflection r(-)) coefficient. The impedance tube apparatus is commonly used for the characterization of locally reacting material samples. The sound absorption determination by ITM can be done by measuring maximum and minimum pressure amplitude in the tube by means of the moving microphone probe (the method using the standing wave ratio, as described in [28]), or by determination of the pressure transfer function between wave components at two or more microphone positions at a given distance from the specimen along the tube [29]. The disadvantage is that the ITM does not allow for oblique incidence measurement. Another standardized laboratory method which is used very often is to determine the statistical sound absorption coefficient α_S(-) in a diffuse field in a reverberant room, according to ISO 354 [30]. The test results obtained by this method are often considered the more realistic for characterizing specimen absorption properties in situ, as compared to the ITM approach. However, this method requires a reverberant room and a flat specimen with a total surface of 10–12 m^2. From this expensive measurement procedure "just" the absorption coefficient is obtained (and not a complex valued reflection coefficient, as is the case in the ITM) and the measurement uncertainty is relatively high. The absorption coefficient is determined based on Eyring's formula and is dependent on the reverberation time measured in the reverberation room with and without the specimen, the room volume and the surface area of the specimen. There are several microphone or p-u probe free-field methods. The basic principles are explained in, e.g., Cox and d'Antonio [31]. Methods differ regarding the required sample size, wave decomposition methods, measurement setup composition and procedure (number of microphones—from two to array, distance of microphones from specimen, angle of incidence, distance of source, etc.). Free-field methods consider the incident sound wave as a plane wave (implying that a well-defined acoustic field is required, demanding the absence of spurious reflections and edge-diffracted waves [32]). A good accuracy can be achieved by means of free-field methods in the frequency range above 290 Hz (for oblique incidence above 400 Hz [33]). Champoux and L'esoerance [34] found that the measurement does not yield accurate results for low values of kR (for R = 3 m and $k < 5.5$ m^{-1}), where k is wave number and R is the distance of the sound source from the specimen surface. They also found that phase mismatch between microphones plays a crucial role, especially in the measurement of low frequencies or highly reflective materials. Assuming the non-standardized, impulse-response based microphone methods, the work of Nocke's [35] can be mentioned, which describes a method to determine the sound absorption from frequency 80 Hz onwards considering Fresnel zones. A different technique for sound absorption determination, by means of a p-u probe where the measured sound pressure and the normal component of the particle velocity determines the absorption, was introduced for the first time by Liu and Jacobsen [36].

Several approaches exist to determine the sound transmission loss. The simplest, which are the same as in the sound absorption case, make use of ITM. For example, the three-microphones method to measure the high *nTL* (up to 100 dB) acoustic samples was developed by [37] (the usual limit is around 50 dB in the frequency range below 500 Hz [38]). Generally, all ITM methods can be divided into two groups: the first group is based on the wave decomposition (WD) (three or more microphones, one or two acoustic loads) and the second group is based on the transfer matrix (TM) method (one or two acoustic loads). The disadvantage of ITM methods, similarly as in the case of sound absorption determination, is that the size of the test specimen is non-realistically small (which causes problems in relation to the way the test specimen are fitted in the tube)

and the TL is determined under normal-incidence acoustic waves only (nTL). There are several standardized methods to test "real-size" specimens. For example, the most often used laboratory methods are in accordance with ISO 10136-2 [39]. The method is intended to determine the airborne sound insulation R of separating structures mounted in the transmission suite. In this approach, it is required that sound transmission via flanking paths is suppressed sufficiently well and the sound field in the source and receiving room are assumed to be diffuse. The spatially averaged sound pressure level in the source and receiving room are measured by a microphone, and the contribution of the reverberant sound field to the total measured sound field in the receiving room is accounted for. The less popular and alternative laboratory technique follows the standard ISO 15186-1 [40] where the intensity sound reduction index R_I is determined based on averaged sound pressure level in the source room, and the sound intensity level radiated from specimen surface in the receiving room. In this approach, the radiated intensity levels are determined by means of a sound intensity probe, and the receiving room is preferably an anechoic room. For in situ measurements, the standards ISO 16283-1 [41] and ISO 16283-3 [42] for airborne sound insulation of walls, small elements and facades, respectively, were established. Similar to the case of laboratory measurement, the intensity method exists for in situ cases [43]. To cope with the high measurement uncertainty of the sound reduction index measurements of building elements in the laboratory according to standards, at low frequencies, two alternative measurement approaches were developed. The first one is a measurement procedure in which a diffuse field is created in the source room through positioning an array of loudspeakers close to the specimen to be excited in the near field [44]. The structural response measurement was done by means of vibrometry (laser Doppler vibrometer, LDV). The second one is a hybrid experimental numerical approach to determine airborne sound insulation by using mobility measurement combined with a numerical procedure [45]. In this approach the device under test is mechanically excited by means of a shaker, and the response is measured by LDV. An alternative approach is to excite the structure by means of a Nd:YAG pump laser [46]. This measurement method has the advantage that the excitation is done contact-less, yielding a contact-less approach for both excitation and response measurement, which would have advantages for application in situ.

The sound absorption coefficient as well as sound transmission loss can be determined by different methods relating to the type of acoustic field and source. The application of the vibrometry technique has already proved its usefulness in building acoustics several times. Vibrometry generally helps for better understanding the structure's behaviour in the low frequency range. In the literature, one can find already the scanning laser Doppler vibrometer application for a normal incidence sound absorption determination (for high frequency range—above 3 kHz) [47]. However, the reflection coefficient was determined based on a number of Doppler frequency shifts measurements at different laser beam angles obtained by scanning the field of the standing wave tube made from glass (during operation with the test specimen), backed by a rigid wall with retroreflective tape, which is very far from the technique numerically investigated in this article.

Despite of the wide range of the measurement approaches briefly mentioned above, in this article, we focus on the determination of the acoustic properties (sound transmission loss nTL transmission coefficient τ(-) and acoustic absorption α(-)) of membrane-type specimens excited by well-defined plane wave excitation by means of surface displacement (in the impedance tube environment). Numerical models were used to simulate the membrane-type specimen being mounted in an impedance tube. Both properties were determined by means of incident pressure and specimen surface mobility information under normal incidence plane wave excitation. The data processing procedure yields both α and τ. However, because these two quantities are related to each other (as will be discussed in Section 2, near Equations (6)–(8)), emphasis is put on the determination of the transmission coefficient τ. Subsequently, the proposed method was experimentally tested.

By combining the known incident sound power and the frequency response of the average surface mobility, both acoustic characteristics can be determined for normal incidence plane waves. The paper is outlined as follows: Section 2 Materials and Methods including the theoretical explanation of the approach used for the determination of nTL, α and τ and the numerical study focused on theoretical verification for two different specimens and six different boundary scenarios. In the Section 3, the laboratory experiment is introduced. Subsequently, numerical simulations and experimental results were analysed (Section 4). This work should be considered as an intermediate step towards a method to measure the acoustic characteristics of membrane structures (e.g., tent structures) in situ.

2. Materials and Methods

2.1. Theory

2.1.1. Determination of Normal Incidence Sound Transmission Loss

The normal incidence sound transmission loss nTL (dB) is defined as the ratio of the incident and transmitted sound power (Watts), or by means the sound transmission coefficient τ(-) using the ITM. The transmitted and incident sound power (W_t and W_i) need to be derived from measurements in the impedance tube. Generally, the most accurate technique to determine nTL is the measurement approach based on the transfer matrix ™ approach, precisely described in ASTME2611-09 [48] and ISO 10534-2 [29]. An application of the method described in the standard is given in [49]. The method requires the determination of the transfer matrix by means of a measurement of the complex sound pressure (amplitude and relative phase) at four locations, two on either side of the specimen.

$$nTL = 10log_{10}\left(\frac{W_i}{W_t}\right) = 10log_{10}\left(\frac{1}{\tau}\right) = 20log_{10}\left|\frac{T_{11} + \left(\frac{T_{12}}{\rho c}\right) + \rho c T_{25} + T_{22}}{2e^{jk_0 d}}\right| \quad (1)$$

where W_i, W_t, τ, k_0, c, d, and ρ are incident and transmitted sound power (Watts), transmission coefficient (-), wave number (m^{-1}), speed of sound (m/s), diameter of the tube (m), density of the air (kg/m^3) and T_{11}, T_{12}, T_{21}, T_{26} are transfer matrix elements derived from transfer functions between sound pressure measured at the microphone positions, respectively. Usually, two different terminations (anechoic, open, minimally reflecting, etc.) are used. In specific cases, when the specimen is geometrically symmetrical and is presenting the same physical properties to the sound field on both sides, the one-load method is sufficient for use. When using this method, the effect of reflections from the termination is almost negligible. For more information about the measurement procedure, see standard ASTME2611-09 [48]. Later, a modification of the method was developed for just three microphone measurements (two in the upstream part of the impedance tube, third microphone flush mounted directly on the hard termination) [50].

Another possible method to determine nTL is based on wave decomposition (WD) theory, which deals with complex wavefields upstream and downstream of the element. The goal of the method is to decompose the wavefields in terms of forward and backward propagation waves. The method went by several modifications from three microphones (two flush mounted upstream and one downstream) developed by Seybert and Ross [51] to four microphones (similarly mounted as in the TM approach) developed by Chung and Blaser [52,53]. Later, the WD-TM hybrid method was developed by Bonfiglio and Pompoli [54]. They proposed a one-termination measurement approach based on a transfer matrix formulation, taking into account the reflection contribution from the end termination and the phase shift introduced by the material. The two mentioned WD methods assume a fully anechoic termination. From the WD methods, the best results might be achieved by an approach developed by Salissou [55], whose work was influenced by Ho et al. [37], and Peng et al. [56] as well. The method takes into account the complex reflection coefficient at the surface of the sample on the source side and on the termination side (r_1 and r_2) as well as the complex reflection coefficient at the surface of the termination r_b. As the reflection coefficient r_2 can be derived just by combining two terminations measurement data, this

measurement technique requires two terminations (read more about in [55]). The normal incidence transmission loss can be subsequently derived as (Equation (2)).

$$nTL = -20log_{10}\left|H_{32}\left(1 - r_2 r_b e^{2jk_0 D_2}\right)\frac{e^{jk_0 L_1} + r_1 e^{-jk_0 L_1}}{e^{-jk_0 L_2} + r_b e^{jk_0 L_2}}\right| \quad (2)$$

where H_{32}, D_2, L_1, L_2 and j is the transfer function between microphones 2 and 3, the distance between the termination and the sample, the distance between microphone 2 and the sample on the source side and microphone 3 and the sample on the termination side, respectively, and imaginary unit (Figure 1).

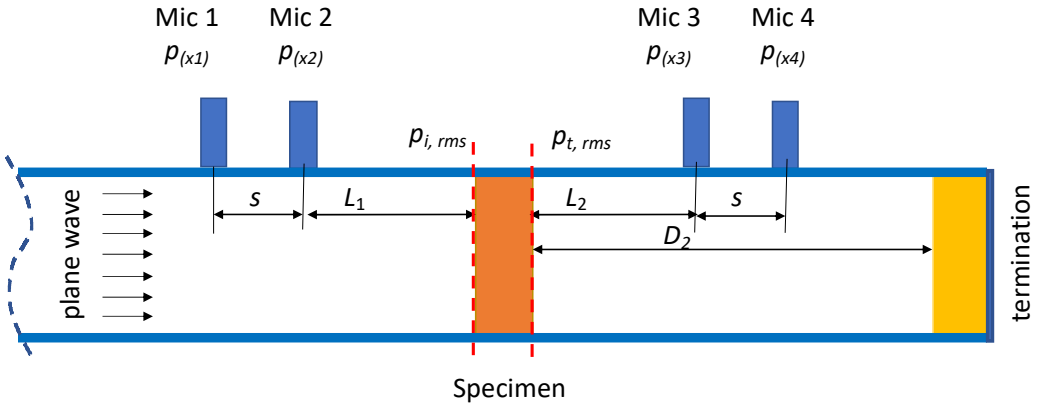

Figure 1. The scheme of the impedance tube with indication of all necessary variables to determine *nTL*. Upstream tube (Left), downstream tube (Right). Where $p_{(x1–4)}$ and Mic 1–4 denote the microphone positions, where the sound pressure is measured related to the x-coordinate, $p_{i,rms}$ and $p_{t,rms}$ are effective values of the incident and transmitted sound pressure at the surface of the specimen (derived from the measurement data $p_{(x1–4)}$), s is distance between microphone positions and L_1, L_2 are distances from of the microphone to the specimen surface.

An interesting approach was recently developed by Wei [57], who proposed the WD-based *nTL* method using only two upstream microphones (the so-called upstream tube wave field decomposition UWD).

One of the methods that is used in this paper as a reference for the determination of *nTL* was derived from the work by Seybert [58]. Unlike other methods, it takes into account the multiple reflection form the back of the impedance tube. The method was developed originally for the sound transmission loss determination in ducts systems (Equation (3)).

$$nTL = 10log_{10}\frac{S_{11} + S_{22} - 2C_{12}cosk_0 s + 2Q_{12}sink_0 s}{S_{33} + S_{44} - 2C_{34}cosk_0 s + 2Q_{34}sink_0 s} \quad (3)$$

where S_{11}, S_{22}, S_{33}, and S_{44} are auto spectra (Pa^2) of the total acoustic pressure at microphone positions 1, 2, 3 and 4 (Figure 1), Q_{12} and Q_{34} are imaginary parts and C_{12} and C_{34} are the real parts of pressure cross spectra between microphones 1 and 2 or 3 and 4 and s (m) is distance between microphone pairs 1 and 2 or 3 and 4, respectively. The method is precisely described in Reference [58].

Thus far, an overview of several of the most well-known methods for *nTL* determining has been mentioned. As mentioned earlier, motivated by the idea of Martens et al. [5], the presented work wants to prove the theory that if the incident sound pressure and the vibration vector of membrane measured by means of the chosen vibrometry technique is known, the sound transmission loss as well as absorption can be determined. In the case of an impedance tube, the radiated sound power into the downstream part of the tube, or the sound pressure at a specific distance from the vibrating surface (depending on the termination), can be determined from the spatially averaged measured displacement of

the vibrating surface. The normal component of the wall velocity is equal to the particle velocity at the wall surface in the case of the perpendicular plane wave excitation [59]. The measured specimen can be considered as a non-baffled piston, assuming a simple $\rho \cdot c$ impedance. Motivated by the work of Chen [20] (hereinafter referred to as the Mobility-based Method—MM), the sound transmission loss can be subsequently determined as (Equation (4)):

$$nTL = 20log_{10}\frac{p_{i,rms}}{|j \cdot \omega \cdot \rho_0 \cdot c_0 \cdot \langle w \rangle|} \quad (4)$$

where <*w*> is the spatially averaged displacement measured at the specimen surface at the receiving side, $p_{i,rms}$ (Pa) is the rms value of the incident sound pressure at the *z*-coordinate of the upstream side of the specimen, c_0 is speed of the sound (m/s) and ρ_0 density of the air (kg/m^3). The above described method, which combines measurement data of the membrane displacement as measured by means of a laser Doppler vibrometer and the sound pressure measurement data of two microphones at the source-side of the impedance tube, is referred to as the mobility-based method (MM). The mobility-based measurement method proposed in this paper, was motivated by the work of Tijs [60] as well as Chen [20]. The same principle was used for the sound absorption determination (see Section 2.1.2).

The application of this procedure can be found in membrane analysis, when the specimen is accessible only from the acoustic excitation side (laboratory or in situ) specially in the cases when the surface of investigation in inaccessible places due to location or extreme conditions. In case of access from the receiving side, the application can be applied for planar specimen without limitations. The comparison with methods mentioned above (Seybert, Salissou and ASTM E261109) and below (ISO 10534-2) can be found in Sections 4 and 5.

2.1.2. Determination of the Normal-Incidence Sound Absorption and Transmission Coefficient

As mentioned above, the transfer function method (TFM) in accordance to ISO 10534-2 is the approach most often used for determination of the sound absorption coefficient in practice [29]. The method uses an impedance tube with a sound source connected to the one end of the tube and the test sample fixed in the tube at the other end. The complex sound pressure is measured by means of two flush-mounted fixed microphone positions in front of the specimen. The complex reflection coefficient *r* can then be determined by means of the acoustic wave field interference decomposition. The sound absorption coefficient (α(-)) (Equation (5)) as well as other quantities like surface impedance (*Z* (Pa s/m)) and admittance (*G*(-)) of absorbing materials can be derived subsequently. The acoustic waves generated by the source below the cut-off frequency of the tube may be considered as plane waves.

$$\alpha = \frac{W_a}{W_{in}} = \frac{W_q + W_T}{W_{in}} = 1 - |r \cdot r^*| = 1 - |r|^2 = 1 - \left| \frac{\frac{p_{(x2)}}{p_{(x1)}} - e^{-jk_0 s}}{e^{jk_0 s} - \frac{p_{(x2)}}{p_{(x1)}}} e^{2jk_0 x_1} \right|^2 \quad (5)$$

where *r**(-) and *s* (m) are complex conjugate of the reflection coefficient and the distance between microphone positions 1 and 2, $p_{(x1)}$, $p_{(x2)}$ and k_0 is sound pressure at coordinate x_1 (m) and x_2 (m) and wave number (m^{-1}) (Figure 2).

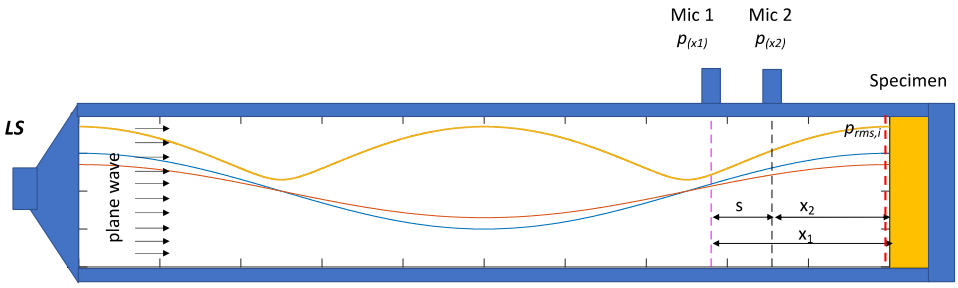

Figure 2. Scheme of determination of the sound absorption by means of an impedance tube. The curves indicates the amplitude of incident (blue curve), reflected (red curve) normal incidence plane wave and the standing wave ratio (yellow curve). Where $p_{(x1–2)}$ and Mic 1–2 denote the microphone positions, where the sound pressure is measured related to the x-coordinate, $p_{rms,I}$ is effective values of the incident sound pressure at the surface of the specimen (derived from measurement), s is distance between microphone positions, x_1, x_2 are distances from of the microphones 1 and 2 to the specimen surface, respectively, and LS is loudspeaker.

The measurement method proposed in this paper combines the laser doppler vibrometer and microphone measurement data (i.e., the surface displacement and known incident pressure $p_{rms,1}$ at the plane at the surface of the specimen—specifically a membrane). The sound transmission and the absorption coefficient of the membrane are closely related. Whilst in Section 2.1.1 it was already detailed how the sound transmission nTL can be determined from sound pressure and vibration measurements, the absorption coefficient α can also be determined in this way, as explained below. The sound absorption coefficient is defined as a ratio of energies (Equation (5)), where W_a, W_{in}, W_q, W_T in (W) are, respectively, the absorbed sound power, incident sound power, dissipated sound power in the membrane and the transmitted sound power. Whereas the sound absorption in porous materials is caused by viscous and relaxation losses, in stretched membrane resonates it depends on the material properties, tension and the geometry of the membrane. If the excitation of the membrane is low (and non-linearities are neglected), the dissipation caused by dissipation of vibration energy (into heat) is also negligibly low. Therefore, in case of nonperforated membranes, the dissipation of energy out of the resonance region can be in most of cases neglected. The observed decrease in the sound reflection spectra is mainly related to the high sound transmission at the membrane resonance frequencies. By neglecting the dissipated energy in the membrane (which is often valid in the case of the single, thin membranes without internal dissipation), the absorption can be approximated by τ(-), as defined by Equation (6):

$$\tau = \frac{W_T}{W_{in}} \approx \frac{(\omega \cdot \rho_0 \cdot c_0 \cdot \langle w \rangle)^2}{p_i^2} \tag{6}$$

where W_T and W_{in} are the transmitted (obtained from the surface mobility at the receiving side of specimen) and incident sound power in (W) at the specimen surface and p_i is the sound pressure at the surface of incidence and can be expressed as (Equation (7)):

$$p_i = \frac{p_{(x_1)} e^{-jk_0 x_1} - p_{(x_2)} e^{-jk_0 x_2}}{e^{-2jk_0 x_1} - e^{-2jk_0 x_2}} \tag{7}$$

where $p_{(x1)}$, $p_{(x2)}$ and k_0 is sound pressure at coordinate x_1 (m) and x_2 (m) and wave number (m^{-1}), respectively. The pressure data $p_{(x1)}$, $p_{(x2)}$ can be obtained by the two microphones at the source side of the impedance tube.

From the above mentioned the sound absorption can be derived (Equation (8)). The equation is valid only for the perpendicular plane wave excitation of the specimen with negligible low internal losses (ideal membrane).

$$\alpha \approx 1 - \left| \frac{p_{i,rms} - (j \cdot \omega \cdot \rho_0 \cdot c_0 \cdot \langle w \rangle)}{p_{i,rms}} \right|^2 \quad (8)$$

2.2. Description of Numerical Study

2.2.1. Single Layer Membrane Sample

A 3D Finite Element Analysis (FEA) model that includes acoustic-structure interaction was created in the commercial software COMSOL Multiphysics to simulate the surface mobility of a membrane mounted in an impedance tube. Based on the simulation data, the *nTL*, α and τ were determined using the theory that was presented in the previous chapter. To resemble the real case, the situation of a membrane being mounted in an impedance tube, the FEM model of impedance tube with inner diameter of the cylinder shape tube was d = 0.1 m created ($d < 0.586^{*}c/f_{upper\ frequency\ limit}$, which corresponds to the upper frequency limit, or the cut-off frequency of 2 kHz). The distance between microphones (receiving datapoints) was set to s = 0.075 m ($s << c/(2^{*}f_{upper\ frequency\ limit})$).

The upstream and downstream impedance tube is a cylindrical tube with acoustically hard wall boundary conditions. The model allows for a variation of the surface impedance of the tube termination (backing wall), with the impedance $Z = (1 + r)/(1 - r) \times (\rho \cdot c_0)$, where r is the desired reflection coefficient of the backing wall. As the testing specimen, a 0.5 mm thin membrane with material properties of PTFE (Polytetrafluoroethylene) foil was chosen. PTFE is widely used in modern architecture to cover open spaces. It is also used as a façade-coating material.

The membrane was clamped at the perimeter. The tension was applied as initial stress in the radial and tangential directions of the membrane as T_0 = 10 kN/m^2. The Young's modulus, Poison's ratio, and density of the PTFE membrane were 4.8125 $\times$ 10^9 Pa, 0.33 and 2175 kg/m^3, respectively. The structural loss factor was defined as η_s = 0.02(-) (for objective reasons related to the use of linear solvers, it was necessary to enter at least minimal damping into the model). The membrane was surrounded by air (ρ_0 = 1.29 kg/m^3; c_0 = 343 m/s) at both sides of the membrane and was excited in by a 1 Pa plane wave radiated from the upstream end of the tube. Six absorption properties of termination were simulated (α_1 = 1.0; α_2 = 0.9; α_3 = 0.7; α_4 = 0.5; α_5 = 0.2; α_6 = 0.1), to investigate the impact of the termination on the resulting *nTL*, τ and α, respectively. The generated mesh resulted into 34,547 degrees of freedom (DOF) with a maximum element size ($c_0/f_{upper\ frequency\ limit}/5$) $\cong$ 0.034 m (Figure 3a).

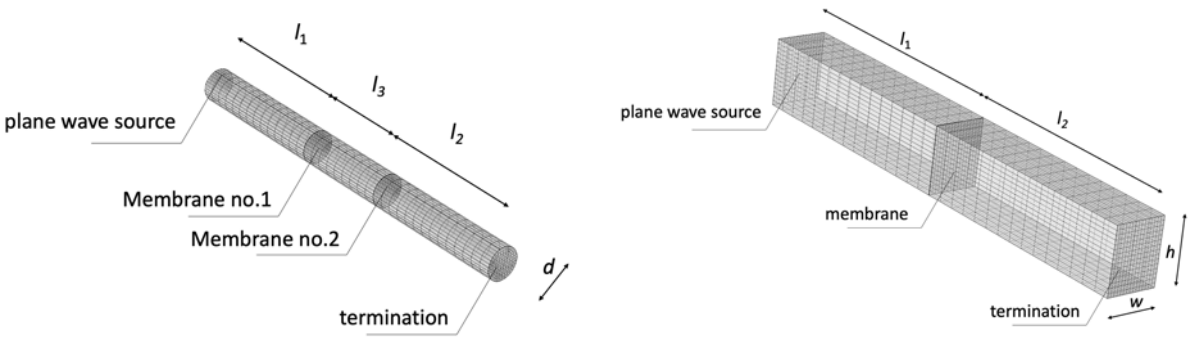

(**a**) (**b**)

Figure 3. View of 3D FEM model meshing. (**a**) Single membrane; (**b**) rectangular shape membrane, where l_1, l_2, h, w, d are length of downstream and upstream part of impedance tube, height, width and diameter of the tube cross section, respectively.

2.2.2. Rectangular Shape Membrane Specimen

Despite the experience that the cross section of the impedance tube is almost always a circle, an additional study with a rectangular shaped membrane was performed. The reason was that in the realization of building structures one seldom encounters circular-shaped membranes. The change in shape should introduce additional resonant areas into the membrane response. For this purpose, a model of an impedance tube with dimensions in the cross section of 100 × 125 mm with a membrane thickness of 0.5 mm (PTFE foil) was created. The tension, Young's modulus, Poison's ratio, structural loss factor and density of the PTFE was set similar to the case with one membrane. Again, six absorption properties of termination were simulated (α_1 = 1.0; α_2 = 0.9; α_3 = 0.7; α_4 = 0.5; α_5 = 0.2; α_6 = 0.1), to see the impact of the termination on the resulting nTL, τ and α, respectively. For this specimen case, only the ASTM, ISO and Mobility based methods were compared. The generated mesh resulted to 106,430 DOF with maximum size of mesh element ≅ 0.049 m (Figure 3b). It should be mentioned that the upper frequency limit, or the cut-off frequency, is 1372 Hz for this case.

3. Description of Measurements

3.1. Description of Measurement Setup

In this section, the measurement setup and the specimen examined in the study is described. The measurement setup was created based on the impedance tube principle as described in the ASTM or ISO standards [25,44]. The core part of the construction was a set of rigid steel tubes of diameter 0.1 m, which gives us an upper cut-off frequency of about of 2 kHz. To allow an LDV-scan of the vibrating membrane the impedance tube was accessible from one side surface of the chosen specimen. In this paper only the single membrane experiment is presented so the scanning from one side, the muffler side, was sufficient. However, the measurement setup gives opportunity to perform scanning measurements from both sides of the sample (also from the source side). This would find the application in cases of more complex specimen (which were not investigated here). Therefore, the loudspeaker (on the source side) was mounted on the (cylindrical) wall of the impedance tube as shown in Figure 4b.

(**a**) (**b**)

Figure 4. The measurement setup modification description. (**a**) Photo of full setup; and (**b**) the axis perpendicular side connection of LS.

The 6 speaker type "Eminence ME6-7586408 ohm" was mounted on a rigid plate. The speaker was driven by a Mono Power Amplifier (Vincent SP-996). On the other side of the impedance tube apparatus, a low frequency muffler with an open end was mounted. The muffler consisted of a sheet-steel wall-based hollowed cone (upstream diameter = 0.75 m; downstream diameter = 0.1 m; length = 0.97 m), filled with mineral wool (see Figure 4a—

right end). The muffler was designed in accordance to the standards ISO 5136 and ISO 7235 [61,62]. The measured sound absorption of the muffler is shown in Figure 5a. One can see that the sound absorption has a straight tendency as the function of the frequency in the range from 200 to 1100 Hz.

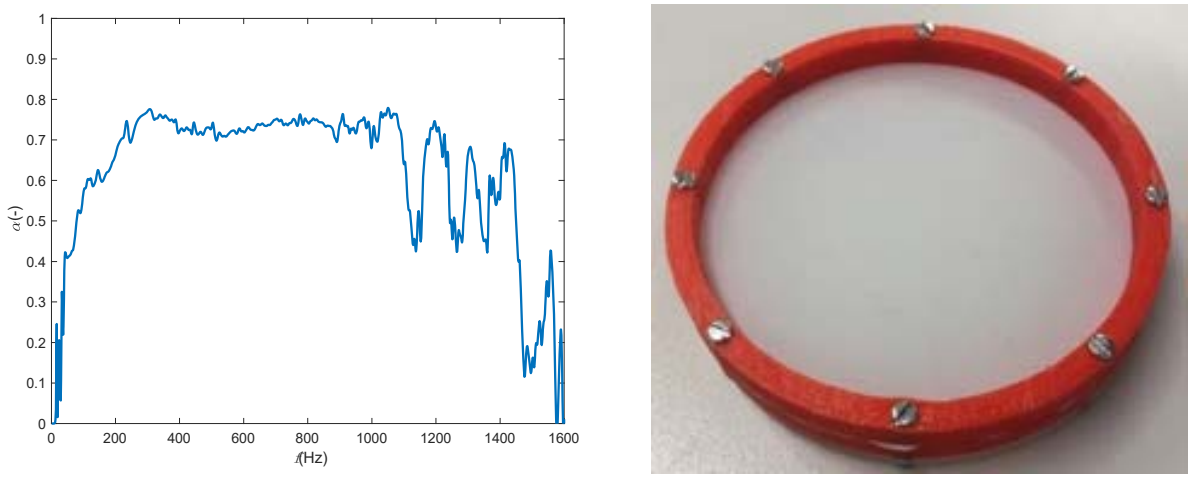

(**a**) (**b**)

Figure 5. (**a**) The sound absorption coefficient spectra of the muffler measured in accordance to ISO 10534-2; and (**b**) test specimens—a single-leaf 0.5 mm PTFE membrane.

Due to this, the presented measurement results were also evaluated only in this frequency region. Several holes were available in the tube apparatus for flush mounting the measurement microphones. The chosen pair distance (for the upstream and downstream part for nTL as well as τ and α determination) was 75 mm in both cases. A scheme of the total setup is shown in Figure 6. The microphones that were used for the measurements were a pair of $\frac{1}{2}$" ICCP pre-polarized microphones (BSWA MA231), conditioned by the multichannel measurement system (Soft db—Tenor 24 bits, 8—channel data-logger). The ASTM and ISO based results were obtained by means of the impulse response measurement. As the excitation signal, for microphone measurement-based methods, a sine sweep was used. The Matlab™ postprocessing routines were created for the data processing.

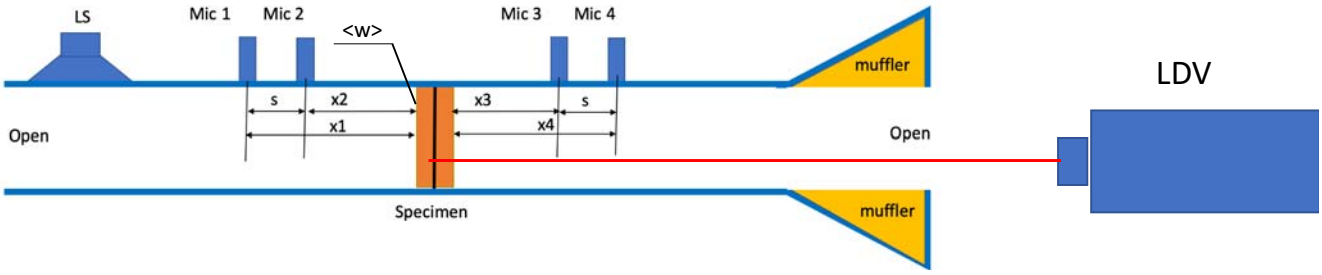

Figure 6. Scheme of measurement setup with LDV scanning head. Where Mic 1–4 denote the microphone positions, s is distance between microphone positions, x_1–x_4 are distance of the microphones to the specimen surface, <w> is the spatially averaged displacement measured at the specimen surface, LS is loudspeaker, LDV is laser doppler vibrometer.

To determine the mobility-based sound transmission loss, a scanning laser Doppler vibrometer Polytec PSV 400 controlled by PSV Acquisitions SW was used. The measuring perpendicular mesh of 253 points was generated by SW tool and scanned. The reference excitation signal for the mobility-based method was pink noise generated by means of portable signal generator type Minirator-MR1 (NTI). The scanning grid used for spatially averaged velocity (or displacement data) consisted of 305 points.

3.2. Specimen Description

The test specimen was a stretched PTFE membrane with a thickness of 0.5 mm and density of 2175 kg/m^3 (Figure 5b). Other material properties were derived from the numerical parametric study and measurements (Young's modulus and Poison's ratio were 4.8125×10^9 Pa, 0.33). The membrane was stretched on a stretching ring made from PLA material precisely printed by means of a 3D printer (Prusa i3 (Anet a8)) and was fixed inside of the impedance tube apparatus by mastic. The stretching ring consisted of two rings connected by means of eight screws. In this way, the rings' perimeter was divided into eight parts with specific stiffness. After mounting the specimen into the impedance tube, the rings were slightly bended, which caused the variation of the stiffness at the perimeter. Specifically, two of the sixteen perimeter parts were significantly affected (the effect on the measured result is discussed in the Section 4). The tension in the membrane was $T_0 = 850$ N/m^2. The value of tension was derived from the numerical parametric study.

4. Results

4.1. The Normal Incidence Sound Transmission Loss (Simulations)

The nTL, τ and α as determined by the different methods (for nTL-Seybert, Salissou, ASTM and the Mobility-Based method, for α-ISO and for τ-Mobility-Based method) were compared. All the methods were compared for the circular shaped single layer membrane. For the rectangular shaped membrane, the Seybert and Salissou methods were considered for reasons of brevity.

Measuring the acoustic properties (nTL, τ and α) in an impedance tube environment serious artefacts can be caused by standing waves in the impedance tube. Obviously, these effects are unwanted in the measurement of the acoustic properties of the sample. As these artefacts are known to be strongly dependent up the acoustic termination of the impedance tube, terminations were considered having six different values of the sound absorption coefficient α of: $\alpha_1 = 1.0$; $\alpha_2 = 0.9$; $\alpha_3 = 0.7$; $\alpha_4 = 0.5$; $\alpha_5 = 0.2$; $\alpha_6 = 0.1$. In a number of cases, a negative nTL was obtained at some frequencies, which is obviously non-physical, and also related to standing waves in the impedance tube. These negative areas are marked by a pale red colour (see figures below). The most accurate method, which does not show a large dependency on the amount of reflection of the backing, was the ASTM method. For this reason the ASTM method with 100% absorption backing wall has been considered as the reference.

Seybert's method, as mentioned above, is a one-load method and its results are dependent on the termination sound absorption (Figure 7a). By increasing the reflection coefficient of the back termination, the spectra of nTL are strongly affected by multiple reflection between the sample and the termination. Due to these effects, this method requires an anechoic termination. The frequency location of "unwanted" dips in the spectra can be predicted from the relation $f_x = n \cdot c_0/(2 \cdot l_2)$, where n, c_0 and l_2 are an arbitrary natural number, the speed of sound in the air, and the length of the downstream tube, respectively. Beside the dips and peaks related to the standing wave modes in the downstream tube, also the dips which are related to the membrane resonances and the peaks which are related to the anti-resonances, are affected. The worst highest and lowest backing absorption are compared to the ASTM method in Figure 7f. Almost negligible peaks/dips in nTL spectra are occurring in case with the 100% absorptive termination (the thick blue curve), showing the real acoustic properties of the membrane structure under test. By decreasing the termination absorption to 20% the differences increased up to 14 dB. The wave decomposition (WD) by Salissou [55] is a two-load method (Figure 7b). The results that are obtained with this method also strongly dependent on the load termination absorption. In order to obtain reasonable results (less artifacts due to resonances in the impedance tube), at least one of the two loads needs to have an high absorptive termination. Nevertheless, the method of Salissou cannot eliminate the effect of the multiple termination reflections effectively. In the worst case with termination absorption ratio 0.2: 0.1 (very

reflective composition), the ΔnTL reaches the differences more than 20 dB in comparison to the anechoic termination.

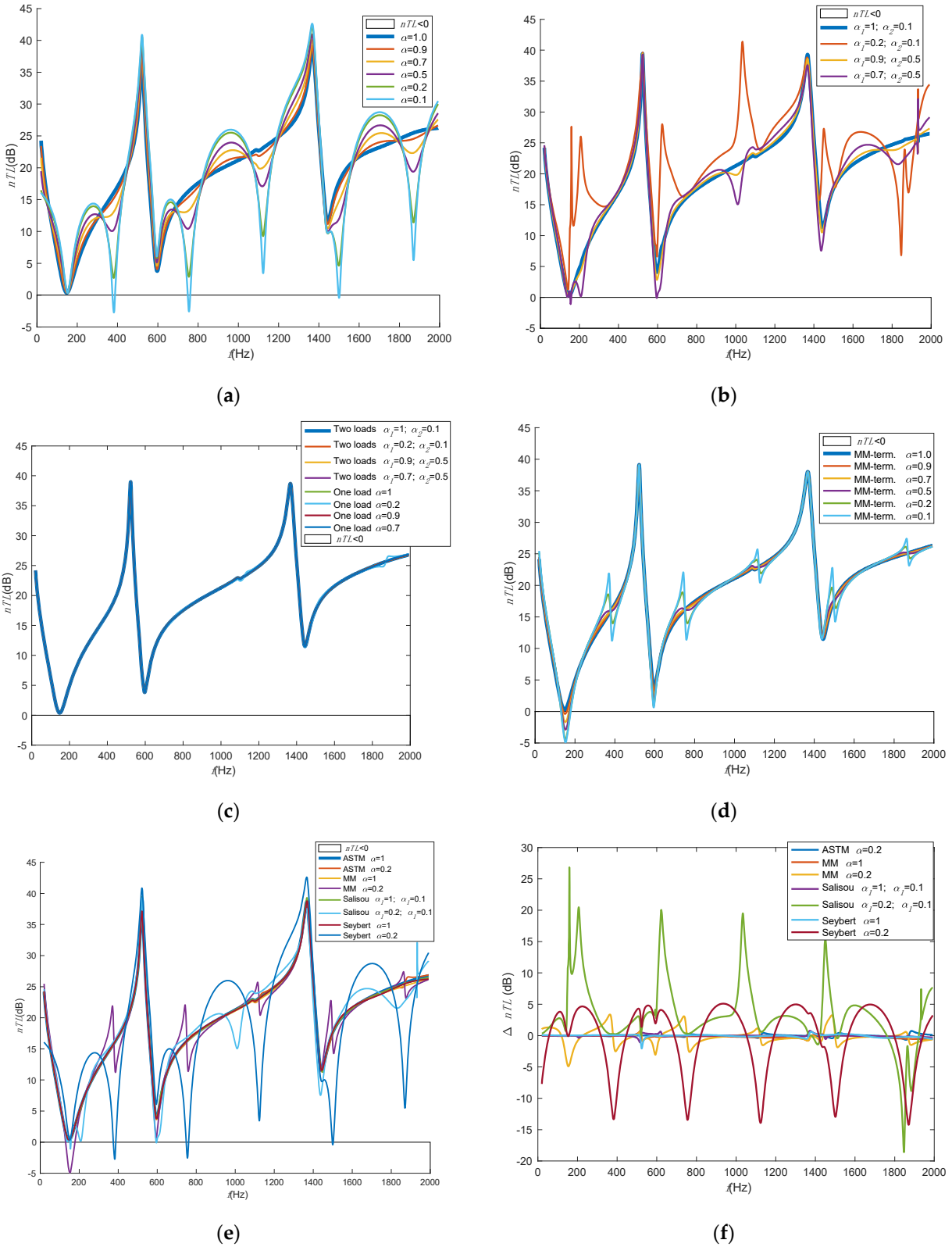

Figure 7. *Cont.*

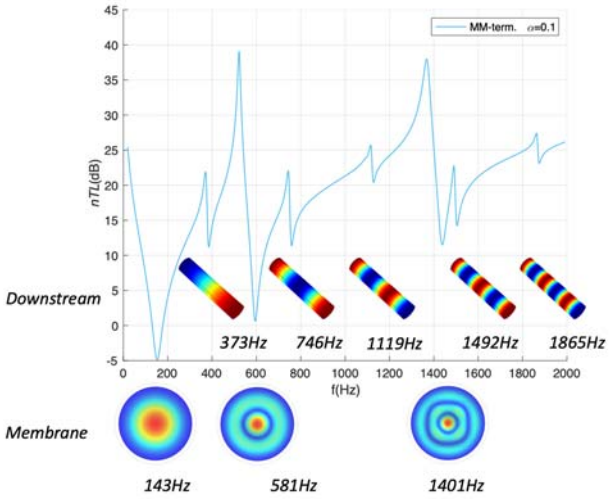

(**g**)

Figure 7. The *nTL* of 0.5 mm thin membrane determination by means of different methods from the FEM model for six different backing wall sound-absorption terminations (variation of termination absorption from α=0.1 to 1). (**a**) Seybert (Wave field decomposition method (WD)—one load); (**b**) Salissou (WD-TM hybrid method—two loads variations with termination ("term." in the legend) absorptions denoted as α_1,α_2 for first load and second load); (**c**) ASTM E261109 ("ASTM" in the legend, Transfer matrix method—single or two-load variations with different termination absorptions denoted as α_1,α_2 for first load and second load variations); (**d**) mobility based method (MM—single load); (**e**) comparison of methods; (**f**) comparison of chosen cases by the difference in the frequency spectra ($\Delta nTL = nTL_i - nTL_{ASTM\ \alpha=1}$); and (**g**) *nTL* spectra of calculated based MM, with termination α = 0.1. The figure also includes structural modes of the membrane as well as the acoustic modes of downstream tube causing the resonant phenomena in the spectrum.

The most accurate method (independent on the termination) for the determination of *nTL* is the method in accordance to ASTM E2611-09 [48] (Figure 7c). Two transfer matrix (TM) methods (single or two loads method) are described in the standard. In the case of a phase synchronized and amplitude calibrated system, the two-loads method can properly and accurately determine *nTL* while effectively neglecting the influence of the backing wall termination on the sound absorption. The single-load method, for the numerical case when the model was perfectly geometrically symmetric, gave reasonably accurate data (comparable with the two-load method). The single-load method can be slightly affected by a high reflection of the termination (Figure 7f). In the worst case for the single layer membrane, the effect was not more than 0.7 dB at specific frequencies.

The results obtained by means of the mobility-based method (MM) are presented in Figure 7d and a comparison with the ASTM method is shown in Figure 7e,f. In this comparison, the ASTM method with an absorption factor α = 1 was chosen as a reference as this method gives most accurate results. As expected, the results obtained with the MM method are also affected by the multiple back/front reflections in the impedance tube. In case of an absorption of 20% at the impedance tube backing wall, differences up to 4 dB were observed compared to the ASTM (α = 1)-reference method.

Figure 7g present the structural and acoustic modes which influence the dips in the *nTL* spectra. In case of the circular (symmetrical) shaped specimens, only the symmetrical modes are influencing the resulting spectra. The acoustic modes are dependent on the length of the downstream. In order to demonstrate the applicability of the MM method to the modally slightly more complicated shape of membranes, the response of a rectangular membrane was numerically assessed. As in the previous case, a comparison of the results was made only between the ASTM and MM methods (Figure 8). The sound transmission loss and absorption of the rectangular membrane are most affected by the modes that have an odd number of half-wavelengths in the transverse direction of the membrane patch (Figure 8c). As in the previous cases, for the anechoic termination, the spectrum determined on the basis of both methods correlates well with each other in a global sense. Exceptions

occur at specific frequencies which are related to resonances and anti-resonances. Here, visible deviations up to 3 dB occur from the second mode having an odd number of half wavelengths (Figure 8c). Paradoxically, this deviation, as in previous cases of anechoic terminations of the MM method, is due to the fineness of the datapoint mesh on the membrane surface. This can distort the attenuation in the resonant phenomenon. By increasing the reflectivity of the backing wall termination, the front-back reflection in the form of additional peaks in the spectrum is more pronounced.

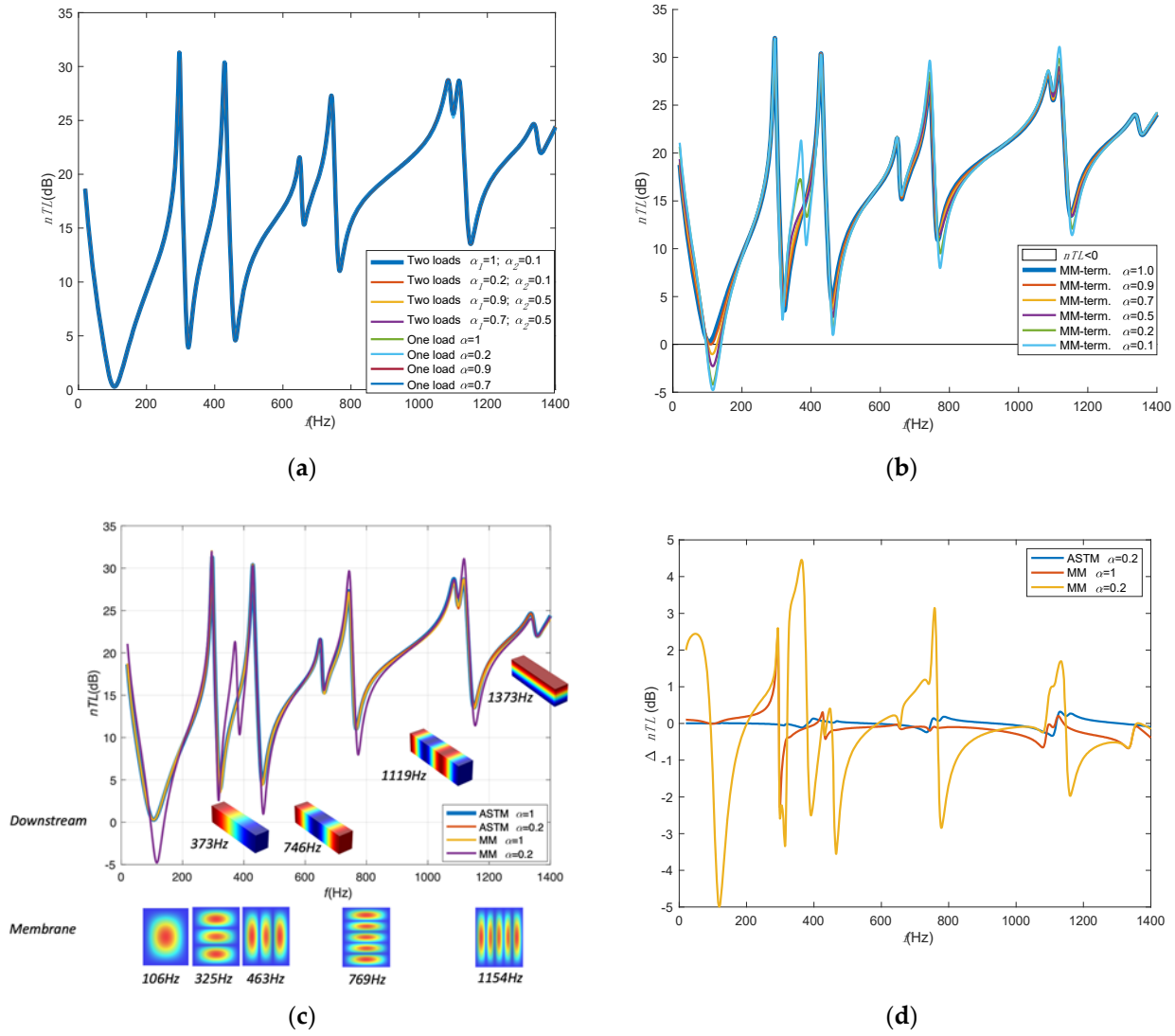

Figure 8. The *nTL* of 0.5 mm thin membrane determination by means of different methods from the FEM model for six different backing wall sound-absorption terminations (variation of termination ("term." in the legend) absorption from α = 0.1 to 1) (**a**) ASTM E261109 ("ASTM" in the legend, Transfer matrix method—single or two-load variations with different termination absorptions denoted as α_1,α_2 for first load and second load variations); (**b**) mobility based method (MM—single load); (**c**) comparison of methods including graphical representation of resonant phenomena causing decreases in the spectrum.; and (**d**) comparison of chosen cases by the difference in the frequency spectra($\Delta nTL = nTL_i - nTL_{ASTM\ \alpha=1}$).

4.2. The Normal-Incidence Sound Absorption and Transmission Coefficients (Simulations)

The normal incidence sound absorption and transmission coefficients were determined by means of two techniques. The first one, the reference method, was the TFM in accordance with ISO 10534-2. The second method, the mobility method, included the surface spatial averaged displacement in the normal direction to the surface (in figures denoted as the

mobility-based method—MM). The comparison of results is shown in Figures 9 and 10. One can see that the results are in both cases dependent on the sound absorption of the impedance tube termination (as expected). For a fully anechoic termination, almost the same results were obtained for both methods. However, reducing the absorption coefficient of the downstream termination the difference of the resulting absorption has increased up to $\Delta\alpha$ = 1(%) to 1.5(%), respectively, where $\Delta\alpha = (\alpha - \tau)\cdot 100\%$, at frequencies of the membrane symmetrical mode resonances. By using the parametric study, one can simply distinguish between the membrane resonance caused absorption/transmission coefficient peaks, the downstream tube termination cased resonances (strong effect in case of single membrane—the increasing effect is visible by increasing the reflection of the termination) (Figure 9a,b).

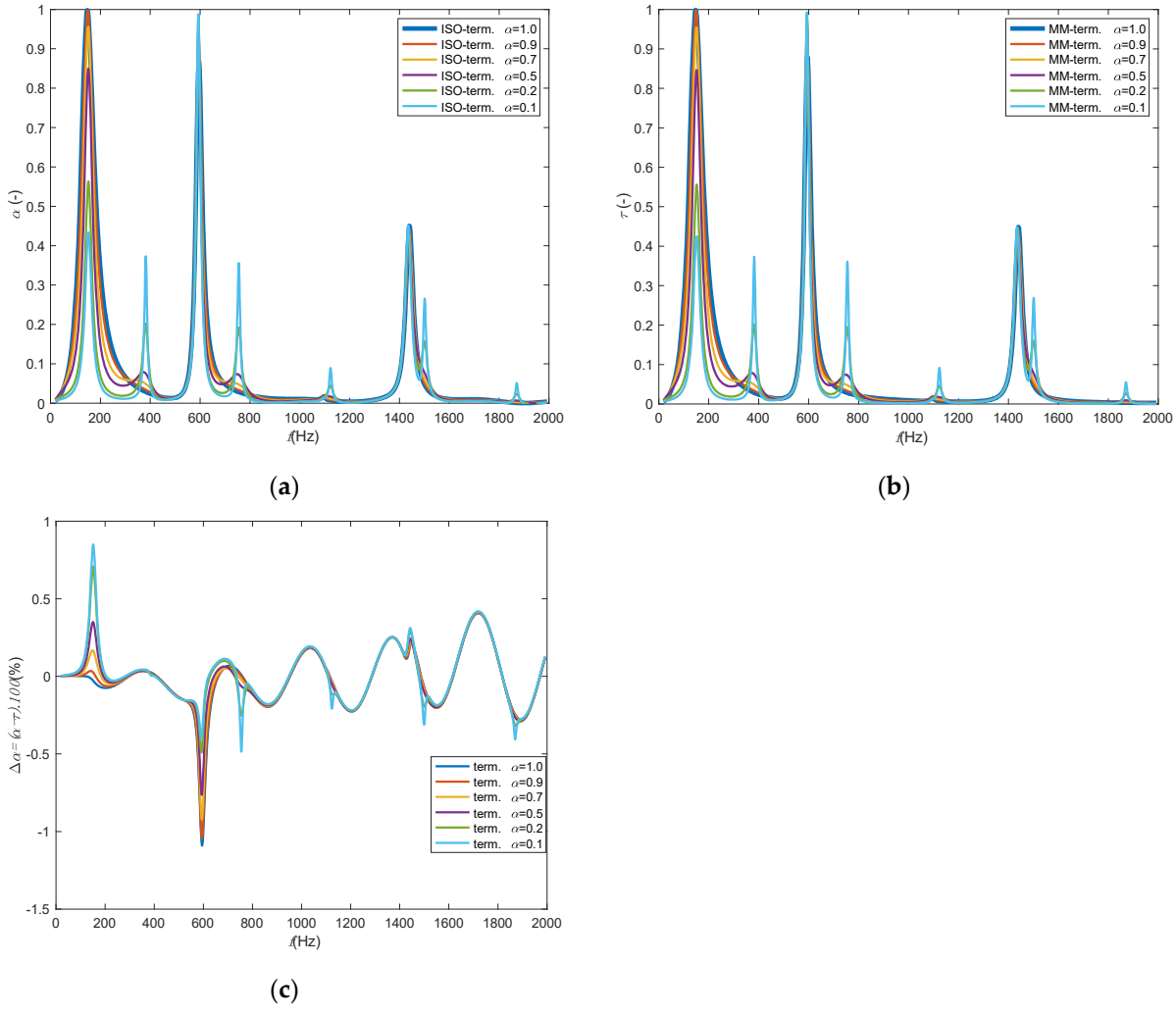

Figure 9. Normal-incidence sound absorption of a single leaf PTFE membrane determined for six different terminations (variation of termination ("term." in the legend) absorption from α = 0.1 to 1, data were obtained from FEM). (**a**) TFM-ISO 10534-2 ("ISO" in the legend); (**b**) mobility-based method ("MM" in the legend); and (**c**) difference between sound absorption obtained by means two methods expressed in percentage.

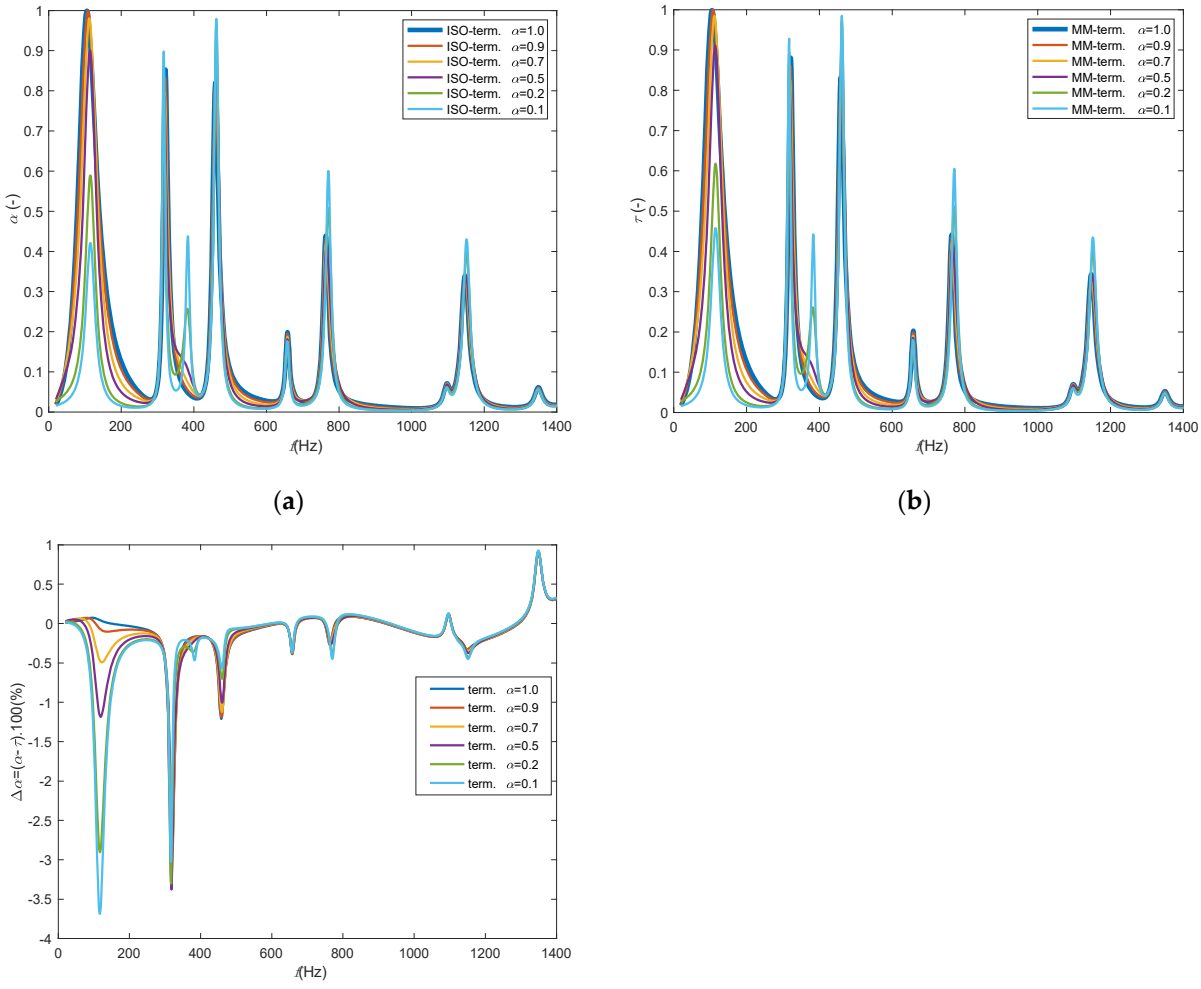

Figure 10. Normal-incidence sound absorption of a single leaf PTFE rectangular shape membrane determined for six different terminations (variation of termination ("term." in the legend) absorption from α = 0.1 to 1, data were obtained from FEM). (**a**) TFM-ISO 10534-2 ("ISO" in the legend); (**b**) mobility-based method ("MM" in the legend); and (**c**) difference between sound absorption obtained by means two methods expressed in percentage.

For a rectangular membrane (Figure 10), resonances caused by downstream front-back reflection are strongly suppressed except for the first mode of the tube, as it occurs near the 3rd and 6th odd membrane modes. The difference in spectra between the individual methods is, unlike the transmission loss (logarithmic expression), expressed as a percentage. Here, again, depending on the type of tube termination, the resonant response manifested in the peak/dip spectrum increases. The deviation with anechoic termination in comparison with MM with the ISO method reaches a deviation of up to 3.5% for the second odd mode and below 1% for other modes, what is acceptable. Interestingly, by changing the shape of the membrane and the associated distribution of resonant modes, an increase in the sound absorption of the sample was achieved.

4.3. Measurement Results

The sound transmission and the sound absorption and transmission coefficient were determined in the impedance tube for the one PTFE foil-based membrane specimens under a plane-wave excitation environment. The mobility method results (*nTL*, α and τ) explained above were compared with results determined in accordance to the ASTM E2611 –09 approach (for *nTL*—single load) and in accordance with the ISO 10534-2 (α). Additionally, the FEM model was created taking in the account the membrane material

properties (see Section 3.1) as well as the measured boundary condition (the tension was T_0 = 850 N/m^2). The resulting comparisons are shown in Figure 11. Additionally, the operation deflection shapes (ODS) of a vibrating membrane related to the chosen frequencies, measured by means of the LDV, are also presented in Figure 11. With focusing to identify the mode shapes, the ODSs are the spatial surface plot of the imaginary part of displacement (the excitation signal was used as the reference signal to acquire information of the phase surface phase).

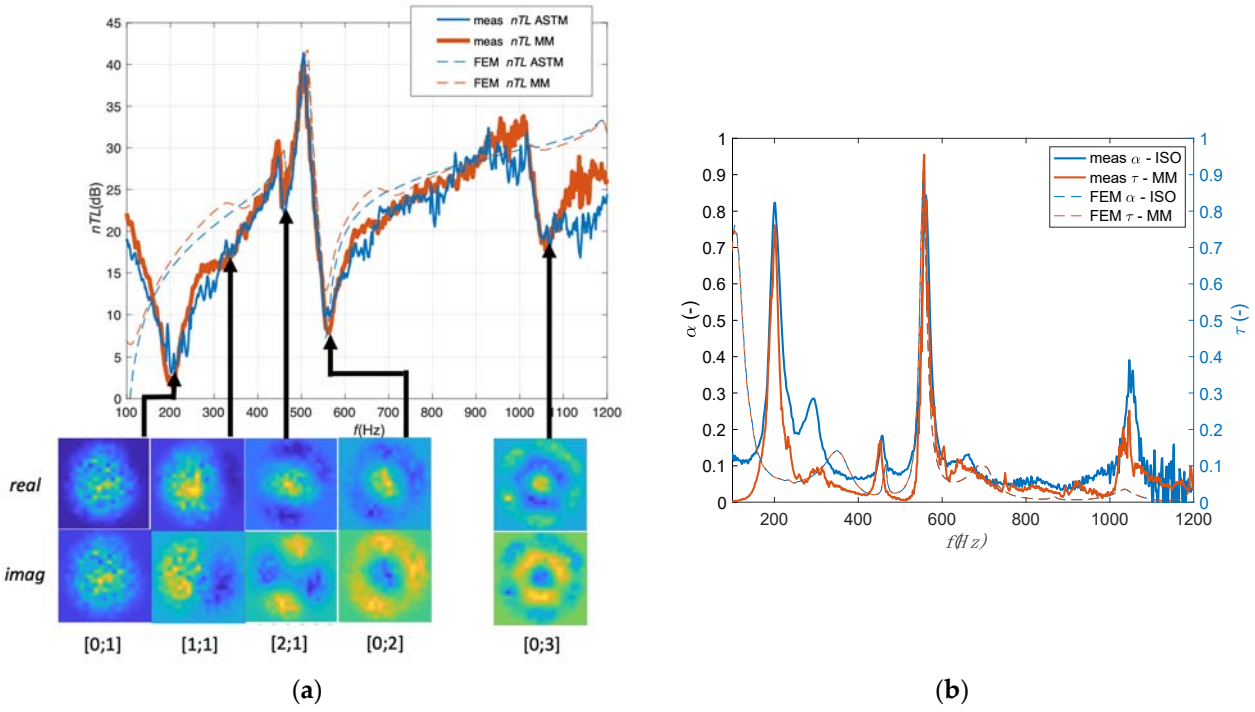

(**a**) (**b**)

Figure 11. (**a**) Sound transmission loss spectra of the single layer 0.5 mm PTFE membrane. (**b**) Measured sound absorption and transmission coefficient s of the single layer 0.5 mm PTFE membrane. Abbreviation describing the measurements based on: ASTM—ASTM E261109; MM—mobility based method; ISO-ISO 10534-2.

The measured *nTL* spectra corresponds to each other rather well. The highest peak of single-membrane *nTL* spectra at a frequency of about 510 Hz is caused by anti-resonance phenomena (the displacement of membrane surface is too low). On the other hand, the dips of *nTL* and peaks of α τ spectra at a frequencies of approximately 205 Hz, 562 Hz and 1078 Hz are caused by structural resonances caused by 1st mode (0.1—the first axisymmetric mode), 4th mode (0.2—the second axisymmetric mode) and the 9th mode (0.3—3rd axisymmetric mode) of the membrane system. Two unexpected dips (that are missing in the idealised simulation cases, e.g., presented in chapter 5.1) in the *nTL* spectra occurs at frequencies 296 Hz and 464 Hz. The dips are related to the 2nd and 3rd structural mode (1.1 and 2.1) of the membrane. Normally, if the membrane edge boundaries would be uniform, the influence of the 2nd and 3rd mode would not be visible. In the experimental case, the stretching ring from PLA material was slightly bent, which affected the stiffness at the membrane edges. The stretching ring consisted of two rings connected by means of eight screws. In this way, the rings' perimeter was divided into eight parts with specific stiffness. After mounting the specimen into the impedance tube, the rings were slightly bended, which caused the variation of the stiffness at the perimeter. Specifically, two of the sixteen perimeter parts were significantly affected. This has been verified also in the FEM tuning process where the significantly lower stiffness (the spring constant k_L was lower by factor 10^4) was needed to set in the boundary system of the membrane clamping. Caused by the already mentioned nonuniformities in the tension in the stretching ring and its bending, that not possible perfectly fit all the investigated frequency spectra. Nevertheless, the FEM

and measurement based obtained results obtained for both discussed methods correspond reasonably well with each other.

Despite the fact that the absorption of the muffler is relatively balanced only in the frequency range from 200 Hz to 1100 Hz, the data from 100 to 1200 Hz were presented in Figure 11. The reason was to demonstrate the effect of the change in the absorption of the termination on the differences in the results. Results comparison of *nTL* spectra is giving similar results in the range from 200 to 1100 Hz. Outside this frequency range, the results differ, which is possibly caused by a high reflection of the muffler that causes unwanted acoustic resonances in the system. The measured and predicted sound absorption spectra show good similarities. The peaks caused by axisymmetric resonance modes have been identified well by both methods. However, the absorption in spectra between first and fourth peak (1st and 3rd axisymmetric mode) differ significantly. In this region the nonsymmetric modes 1.12 and 2.1 are present. The effect of the bending and non-uniform stretching of the membrane possibly increases the interaction between membrane and the ring that causes the resonant interaction and internal loses that were not recognised well by the LDV. This caused the difference between the sound absorption and transmission coefficients.

5. Conclusions

In this article, we focus on the determination of the acoustic properties (sound transmission loss, sound absorption and transmission coefficient) of membrane type of specimens under acoustic plane wave excitation. An overview of the measurement methods to extract the acoustic properties from impedance tube measurement data was given. It was noted that the determination of the acoustic properties (nTL, τ) in an impedance tube environment can be hampered by serious artefacts related to standing waves in the impedance tube. Many measurement methods suffer from this, obstructing the extraction of the real acoustic properties of the test specimen. The nTL measurement method least sensitive on possible backing wall reflection caused by a non-perfectly anechoic termination is the ASTM method (in accordance to standard ASTM E2611-09 [48]). In the case of the membrane sound absorption coefficient measurement, the backing wall impedance is directly influencing the resulting sound absorption. The method recommended by ISO 10534-2 [29] was used as a reference throughout the paper. Subsequently, the theoretical background of the proposed so-called mobility-based method (MM), which combines laser doppler vibrometer measurement data and microphone measurement data, was presented. The proposed MM method was compared with the conventional methods for sound transmission loss and absorption measurement.

The methods were compared using numerically generated data from a finite element model. The FEM models included six different variations of the backing wall termination (α_1 = 1.0; α_2 = 0.9; α_3 = 0.7; α_4 = 0.5; α_5 = 0.2; α_6 = 0.1). The numerical investigation focused on the assessment of the influence of the termination on the resulting values of sound absorption and transmission loss spectra of two differently shaped membranes (single layer circular shaped membrane and rectangular shaped membrane). The proposed mobility-based method was compared with the standardized ASTM (nTL measurement) and ISO (α determination) methods, as well as with two other chosen methods, and the effect of the termination on the sound reflection was assessed. The ASTM method describes a measurement method that uses four microphones and one or two loads (different terminations). When dealing with symmetrical test specimen, only one load suffices.

In the case if two loads method is applied almost no difference in results could be observed. Based on the FEM results, the MM gave similar results for anechoic backing wall termination as the results obtained in accordance to the ASTM E2611-09 with the local deviation up to 3 dB. This is a common phenomenon in numerical modelling, where no or very little damping is defined in the model. In the area of resonance, the results obtained from different domains may be overestimated (in this particular case, the results from the acoustic and the structural domain were compared). In absorption assessment, the deviation is up to 3% for the first membrane resonance frequencies.

At other frequencies the deviation is not more than 1%, for both the absorption factor and the transmission loss. By increasing the reflection of the backing termination, the deviations increases and the effect of the front-back reflection can be recognised. The effect usually did not reach a deviation in the absorption of more than 3% and in the transmission loss no more than 5 dB (excluding the 1st mode resonance effect).

In the experimental part the circular shaped single layer PTFE foil specimen was tested and compared with the FE model fitted to the experiment. The MM was compared with the ASTM (nTL) and ISO (α) measurement methods. The results were presented in narrow band spectra, to see more precisely the differences in the results. The MM method gave reasonable results for nTL spectra. Although the measurement results were affected by the specimen bending caused by mounting in the measurement apparatus, which caused unexpected dips in the spectra, the resulting spectra are comparable. Specifically, the resulting nTL spectra determined in accordance to ASTM and MM correspond to each other rather well. The membrane asymmetrical resonances and anti-resonances (which normally have a dominant effect on the nTL, α and τ spectra) were nicely recognised. LDV gave us the opportunity also to identify other modes of the vibrating membranes. Specifically, in the presented case, when the membrane was not stretched symmetrically (caused by soft bending of the stretching ring—something that would occur often in practice), it was able to determine the reason of occurrence of the additional peaks (dips) in the spectra.

The MM would clearly find application in membranes analysis even for more complicated elements, with higher energy dissipation in the structure and possible internal resonances, the α cannot replace the τ. For practical applications, the advantage of MM is that the nTL as well as α can be determined from a single-sided scan. In case of more complex samples the measurement procedure will be needed to perform from both sides of the specimen.

The method may be extended by a single microphone based incident sound pressure determination approach known from standards. The presented work can be considered as an intermediate step for method development applicable in practice. Main disadvantage of the proposed method has only the limited application and is time consuming in comparison to the conventional methods. The absorption measurement approach can be applied only for membrane-based constructions, specially, with membranes with negligible internal losses. Method is also sensitive on the amount of excitation energy (sensitivity of LDV, respectively). Further investigation in the MM is expected. Future experiments in the anechoic laboratory environment and the in situ free field are essential to prove the wider application of the method. The goal is to have a method appropriate for the determination of membrane-based structures acoustic/structural properties from larger distances. Mainly in the cases when the surface of investigation in inaccessible places due to location or extreme conditions.

Author Contributions: Conceptualization, methodology, software, investigation, resources, writing—original draft preparation, visualization, D.U.; formal analysis, writing—review and editing, D.U., N.B.R. and O.J.; validation D.U., V.J., M.B. All authors have read and agreed to the published version of the manuscript.

Funding: This research was supported by the International Mobility of Researchers in CTU CZ.02.2.69/0.0/0.0/16_027/0008465, CTU project SGS19/166/OHK3/3T/13 Development of modern acoustic measurements and was funded by European Union, grant number H2020-MSCA-RISE-2015 project 690970.

Institutional Review Board Statement: Not applicable.

Informed Consent Statement: Not applicable.

Data Availability Statement: All data included in this work are available upon request by contact with the author Daniel Urbán.

Conflicts of Interest: The authors declare no conflict of interest.

References

1. Paech, C. Structural membranes used in modern building facades. *Procedia Eng.* **2016**, *155*, 61–70. [CrossRef]
2. John, G.; Clements-Croome, D.; Jeronimidis, G. Sustainable building solutions: A review of lessons from the natural world. *Build. Environ.* **2005**, *40*, 319–328. [CrossRef]
3. Urbán, D.; Roozen, N.B.; Zaťko, P.; Rychtáriková, M.; Tomašovič, P.; Glorieux, C. Assessment of sound insulation of naturally ventilated double skin facades. *Build. Environ.* **2016**, *110*, 148–160. [CrossRef]
4. Urbán, D.; Tomašovič, P.; Rychtáriková, M.; Roozen, N.B.; Glorieux, C.H. Sound propagation within a double skin facade and its influence on the speech Privacy in offices. In Proceedings of the Euronoise 2015, Maastrich, The Netherlands, 31 May–3 June 2015; pp. 2543–2548.
5. Martens, M.J.; Michelsen, A. Absorption of acoustic energy by plant leaves. *J. Acoust. Soc. Am.* **1981**, *69*, 303–306. [CrossRef]
6. Strutt, J.W.; Rayleigh, B. *The Theory of Sound*; Macmillan and Co.: London, UK, 1877.
7. Mazumdar, J. A Review of Approximate Methods for Determining the Vibrational Modes of Membranes. *Shock. Vib. Dig.* **1984**, *16*, 9. [CrossRef]
8. Laura, P.A.; Romanelli, E.; Maurizi, M.J. On the analysis of waveguides of doubly-connected cross-section by the method of conformal mapping. *J. Sound Vib.* **1972**, *20*, 27–38. [CrossRef]
9. Wang, C.Y. On thepolygonal membrane with a circular core. *J. Sound Vib.* **1998**, *215*, 195–199. [CrossRef]
10. Wang, C.Y. Vibration of an annular membrane attached to a free, rigid core. *J. Sound Vib.* **2003**, *4*, 776–782. [CrossRef]
11. Ho, K.M.; Cheng, C.K.; Yang, Z.; Zhang, X.X.; Sheng, P. Broadband locally resonant sonic shields. *Appl. Phys. Lett.* **2003**, *83*, 5566–5568. [CrossRef]
12. Huang, T.Y.; Shen, C.; Jing, Y. Membrane-and plate-type acoustic metamaterials. *J. Acoust. Soc. Am.* **2016**, *139*, 3240–3250. [CrossRef] [PubMed]
13. Ciaburro, G.; Iannace, G. Modeling acoustic metamaterials based on reused buttons using data fitting with neural network. *J. Acoust. Soc. Am.* **2021**, *150*, 51–63. [CrossRef]
14. Naify, C.J.; Chang, C.M.; McKnight, G.; Nutt, S. Transmission loss of membrane-type acoustic metamaterials with coaxial ring masses. *J. Appl. Phys.* **2011**, *110*, 124903. [CrossRef]
15. Yang, Z.; Dai, H.M.; Chan, N.H.; Ma, G.C.; Sheng, P. Acoustic metamaterial panels for sound attenuation in the 50–1000 Hz regime. *Appl. Phys. Lett.* **2010**, *96*, 041906. [CrossRef]
16. Naify, C.J.; Chang, C.M.; McKnight, G.; Scheulen, F.; Nutt, S. Membrane-type metamaterials: Transmission loss of multi-celled arrays. *J. Appl. Phys.* **2011**, *109*, 104902. [CrossRef]
17. Yang, M.; Ma, G.; Yang, Z.; Sheng, P. Coupled membranes with doubly negative mass density and bulk modulus. *Phys. Rev. Lett.* **2013**, *110*, 134301. [CrossRef]
18. Sharma, G.S.; Skvortsov, A.; MacGillivray, I.; Kessissoglou, N. Sound scattering by a bubble metasurface. *Phys. Rev. B* **2020**, *102*, 214308. [CrossRef]
19. Yang, Z.; Mei, J.; Yang, M.; Chan, N.H.; Sheng, P. Membrane-type acoustic metamaterial with negative dynamic mass. *Phys. Rev. Lett.* **2008**, *101*, 204301. [CrossRef]
20. Chen, Y.; Huang, G.; Zhou, X.; Hu, G.; Sun, C.T. Analytical coupled vibroacoustic modeling of membrane-type acoustic metamaterials: Membrane model. *J. Acoust. Soc. Am.* **2014**, *136*, 969–979. [CrossRef] [PubMed]
21. Zhang, Y.; Wen, J.; Xiao, Y.; Wen, X.; Wang, J. Theoretical investigation of the sound attenuation of membrane-type acoustic metamaterials. *Phys. Lett. A* **2012**, *376*, 1489–1494. [CrossRef]
22. Zhang, Y.; Wen, J.; Zhao, H.; Yu, D.; Cai, L.; Wen, X. Sound insulation property of membrane-type acoustic metamaterials carrying different masses at adjacent cells. *J. Appl. Phys.* **2013**, *114*, 063515. [CrossRef]
23. Naify, C.J.; Chang, C.M.; McKnight, G.; Nutt, S.R. Scaling of membrane-type locally resonant acoustic metamaterial arrays. *J. Acoust. Soc. Am.* **2012**, *132*, 2784–2792. [CrossRef]
24. Roozen, N.B.; Urban, D.; Piana, E.A.; Glorieux, C. On the use of dynamic vibration absorbers to counteract the loss of sound insulation due to mass-spring-mass resonance effects in external thermal insulation composite systems. *Appl. Acoust.* **2021**, *178*, 107999. [CrossRef]
25. Sharma, G.S.; Sarkar, A. Directivity-based passive barrier for local control of low-frequency noise. *J. Theor. Comput. Acoust.* **2018**, *26*, 1850012. [CrossRef]
26. Fuller, C.R. Active control of sound transmission/radiation from elastic plates by vibration inputs: I. Analysis. *J. Sound Vib.* **1990**, *136*, 1–15. [CrossRef]
27. Sharma, G.S.; Sarkar, A. Directivity based control of acoustic radiation. *Appl. Acoust.* **2019**, *154*, 226–235. [CrossRef]
28. ISO 10534-1. *Acoustics—Determination of Sound Absorption Coefficient and Impedance in Impedance Tubes—Part 1: Method Using Standing Wave Ratio*; International Standards Organization: Geneva, Switzerland, 1996.
29. ISO 10534-2. *Acoustics—Determination of Sound Absorption Coefficient and Impedance in Impedance Tubes—Part 2: Transfer-Function Method*; International Standards Organization: Geneva, Switzerland, 1998.
30. ISO 354. *Acoustics—Measurement of Sound Absorption in a Reverberation Room*; International Standards Organization: Geneva, Switzerland, 2003.
31. Cox, T.; d'Antonio, P. *Acoustic Absorbers and Diffusers: Theory, Design and Application*; CRC Press: Boca Raton, FL, USA, 2016.
32. Kuipers, E.R. *Measuring Sound Absorption Using Local Field Assumptions*; University of Twente: Enschede, The Netherlands, 2013.

33. Kimura, K.; Yamamoto, K. The required sample size in measuring oblique incidence absorption coefficient experimental study. *Appl. Acoust.* **2002**, *63*, 567–578. [CrossRef]
34. Champoux, Y.; L'espérance, A. Numerical evaluation of errors associated with the measurement of acoustic impedance in a free field using two microphones and a spectrum analyzer. *J. Acoust. Soc. Am.* **1988**, *84*, 30–38. [CrossRef]
35. Nocke, C. In-situ acoustic impedance measurement using a free-field transfer function method. *Appl. Acoust.* **2000**, *59*, 253–264. [CrossRef]
36. Liu, Y.; Jacobsen, F. Measurement of absorption with ap-u sound intensity probe in an impedance tube. *J. Acoust. Soc. Am.* **2005**, *118*, 2117–2120. [CrossRef]
37. Ho, K.M.; Yang, Z.; Zhang, X.X.; Sheng, P. Measurements of sound transmission through panels of locally resonant materials between impedance tubes. *Appl. Acoust.* **2005**, *66*, 751–765. [CrossRef]
38. Selamet, A.; Ji, Z.L. Acoustic attenuation performance of circular expansion chambers with extended inlet/outlet. *J. Sound Vib.* **1999**, *223*, 197–212. [CrossRef]
39. ISO 10140-2. *Acoustics—Laboratory Measurement of Sound Insulation of Building Elements—Part 2: Measurement of Airborne Sound Insulation*; International Standards Organization: Geneva, Switzerland, 2010.
40. ISO 15186-1. *Acoustics—Measurement of Sound Insulation in Buildings and of Building Elements Using Sound Intensity—Part 1: Laboratory Measurements*; International Standards Organization: Geneva, Switzerland, 2000.
41. ISO 16283-1. *Acoustics—Field Measurement of Sound Insulation in Buildings and of Building Elements—Part 1: Airborne Sound Insulation*; International Standards Organization: Geneva, Switzerland, 2014.
42. ISO 16283-3. *Acoustics—Field Measurement of Sound Insulation in Buildings and of Building Elements—Part 3: Façade Sound Insulation*; International Standards Organization: Geneva, Switzerland, 2016.
43. ISO 15186-2. *Acoustics—Measurement of Sound Insulation in Buildings and of Building Elements Using Sound Intensity—Part 2: Field Measurements*; International Standards Organization: Geneva, Switzerland, 2003.
44. Roozen, N.B.; Leclere, Q.; Urbán, D.; Kritly, L.; Glorieux, C. Assessment of the sound reduction index of building elements by near field excitation through an array of loudspeakers and structural response measurements by laser Doppler vibrometry. *Appl. Acoust.* **2018**, *140*, 225–235. [CrossRef]
45. Roozen, N.B.; Leclère, Q.; Urbán, D.; Echenagucia, T.M.; Block, P.; Rychtáriková, M.; Glorieux, C. Assessment of the airborne sound insulation from mobility vibration measurements; a hybrid experimental numerical approach. *J. Sound Vib.* **2018**, *432*, 680–698. [CrossRef]
46. Roozen, N.B.; Labelle, L.; Leclere, Q.; Ege, K.; Alvarado, S. Non-contact experimental assessment of apparent dynamic stiffness of constrained-layer damping sandwich plates in a broad frequency range using a Nd: YAG pump laser and a laser Doppler vibrometer. *J. Sound Vib.* **2017**, *395*, 90–101. [CrossRef]
47. Vanlanduit, S.; Vanherzeele, J.; Guillaume, P.; De Sitter, G. Absorption measurement of acoustic materials using a scanning laser Doppler vibrometer. *J. Acoust. Soc. Am.* **2005**, *117*, 1168–1172. [CrossRef]
48. ASTM E2571-09. *Standard Test Method for Measurement of Normal Incidence Sound Transmission of Acoustical Materials Based on the Transfer Matrix Method*; ASTM International: Conshohocken, PA, USA, 2011.
49. Piana, E.A.; Roozen, N.B.; Scrosati, C. Transmission tube measurements on the DENORMS round robin test material samples. In Proceedings of the 26th International Congress on Sound and Vibration, Montréal, QC, Canada, 7–11 July 2019.
50. Salissou, Y.; Panneton, R.; Doutres, O. Complement to standard method for measuring normal incidence sound transmission loss with three microphones. *J. Acoust. Soc. Am.* **2012**, *131*, EL216–EL222. [CrossRef]
51. Seybert, A.F.; Ross, D.F. Experimental determination of acoustic properties using a two microphone random-excitation technique. *J. Acoust. Soc. Am.* **1977**, *61*, 1362–1370. [CrossRef]
52. Chung, J.Y.; Blaser, D.A. Transfer function method of measuring acoustic intensity in a duct system with flow. *J. Acoust. Soc. Am.* **1980**, *68*, 1570–1577. [CrossRef]
53. Chung, J.Y.; Blaser, D.A. Transfer function method of measuring in-duct acoustic properties. II. Experiment. *J. Acoust. Soc. Am.* **1980**, *68*, 914–921. [CrossRef]
54. Bonfiglio, P.; Pompoli, F. A single measurement approach for the determination of the normal incidence Transmission Loss. *J. Acoust. Soc. Am.* **2008**, *124*, 1577–1583. [CrossRef]
55. Salissou, Y.; Panneton, R. A general wave decomposition formula for the measurement of normal incidence sound transmission loss in impedance tube. *J. Acoust. Soc. Am.* **2009**, *125*, 2083–2090. [CrossRef]
56. Peng, D.L.; Hu, P.; Zhu, B.L. The modified method of measuring the complex transmission coefficient of multilayer acoustical panel in impedance tube. *Appl. Acoust.* **2008**, *69*, 1240–1248. [CrossRef]
57. Wei, Z.; Hou, H.; Gao, N.; Huang, Y.; Yang, J. Normal incidence sound transmission loss evaluation with a general upstream tube wave decomposition formula. *J. Acoust. Soc. Am.* **2018**, *144*, 2344–2353. [CrossRef] [PubMed]
58. Seybert, A.F. Two-sensor methods for the measurement of sound intensity and acoustic properties in ducts. *J. Acoust. Soc. Am.* **1988**, *83*, 2233–2239. [CrossRef]
59. Rindel, J.H. *Sound Insulation in Buildings*; CRC Press: Boca Raton, FL, USA, 2017.
60. Tijs, E.; Druyvesteyn, E. An intensity method for measuring absorption properties in situ. *Acta Acust. United Acust.* **2012**, *98*, 342–353. [CrossRef]

61. ISO 5136. *Acoustics—Determination of Sound Power Radiated into a Duct By Fans and Other Air-Moving Devices—In-Duct Method*; International Standards Organization: Geneva, Switzerland, 2003.
62. ISO 7235. *Acoustics—Laboratory Measurement Procedures for Ducted Silencers and Air-Terminal Units—Insertion LOSS, Flow Noise and Total Pressure Loss*; International Standards Organization: Geneva, Switzerland, 2003.